HHS Public Access

Author manuscript

J Am Chem Soc. Author manuscript; available in PMC 2016 March 11.

Published in final edited form as:

J Am Chem Soc. 2015 March 11; 137(9): 3372–3378. doi:10.1021/jacs.5b00182.

B_{12}-Mediated, Long Wavelength Photopolymerization of Hydrogels

Zachary L. Rodgers[†], **Robert M. Hughes**[‡], **Laura M. Doherty**[†], **Jennifer R. Shell**[‡], **Brian P. Molesky**[†], **Alexander M. Brugh**[†], **Malcolm D. E. Forbes**[†], **Andrew M. Moran**[†], and **David S. Lawrence**[†,‡,§,*]

[†]Department of Chemistry, University of North Carolina, Chapel Hill, North Carolina 27599, United States

[‡]Division of Chemical Biology and Medicinal Chemistry, University of North Carolina, Chapel Hill, North Carolina 27599, United States

[§]Department of Pharmacology, University of North Carolina, Chapel Hill, North Carolina 27599, United States

Abstract

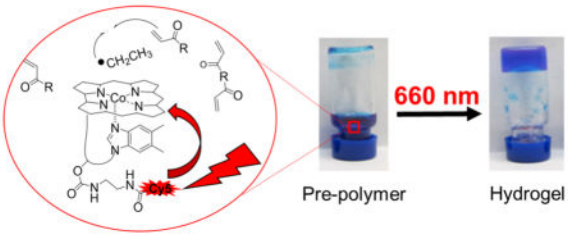

Medical hydrogel applications have expanded rapidly over the past decade. Implantation in patients by noninvasive injection is preferred, but this requires hydrogel solidification from a low viscosity solution to occur in vivo via an applied stimuli. Transdermal photo-cross-linking of acrylated biopolymers with photoinitiators and lights offers a mild, spatiotemporally controlled solidification trigger. However, the current short wavelength initiators limit curing depth and efficacy because they do not absorb within the optical window of tissue (600–900 nm). As a solution to the current wavelength limitations, we report the development of a red light responsive initiator capable of polymerizing a range of acrylated monomers. Photoactivation occurs within a range of skin type models containing high biochromophore concentrations.

INTRODUCTION

Hydrogels are networks of cross-linked hydrophilic polymers that swell in water to many times their dry polymer weight.[1,2] Hydrogel properties mimic the softness and water content

*Corresponding Author: lawrencd@email.unc.edu.

The authors declare no competing financial interest.

Supporting Information

Synthesis and additional photolysis data. This material is available free of charge via the Internet at http://pubs.acs.org.

of natural tissue, making them indispensable tools in tissue restoration and engineering applications.[1,3–5] Indeed, recent reviews have highlighted their expanding clinical use in the treatment of lower back pain,[6] myocardial infarction,[7] cartilage tear,[8] macular degeneration,[9] and drug delivery.[10]

Although a range of chemical and physical gel curing methods exist, in situ cross-linking techniques that allow for injectable hydrogels are of particular interest for clinical use.[11–14] Injection and subsequent gelation confers two distinct advantages over surgical implantation. First, low viscosity solutions can be homogenized with desired cargo and then directly injected into the treatment site. This simplifies the implantation protocol and decreases treatment invasiveness. Second, low viscosity solutions fill the injection sites prior to gelation thereby eliminating the need to know the precise shape of the treatment location.

Many injectable systems, such as those based on poly-*N*-isopropylacrylamides and polyesters, rely on changes in temperature, pH, or redox environment to affect the structure and solvent interactions of the polymer chains to induce physical cross-linking.[15,16] As a result, these systems are oligomer specific and sensitive to changes in gel components creating variability in gelation efficacy, cargo loading, and physical properties.[17] As an alternative, cross-linking via radical photopolymerization offers broad material compatibility, since most synthetic or natural polymers can be modified with radical sensitive acrylates and then covalently cross-linked upon excitation of a radical generating photoinitiator.[5,18,19] In addition, photolithographic techniques coupled to photo-polymerization allow for spatiotemporal control of hydrogel fine structure and properties.[20]

The utility of photopolymerizing injected hydrogel precursors through dermal tissue has been demonstrated.[21,22] Unfortunately, the common α-hydroxyphenyl ketones (Irgacure 2959, λ_{max} < 350 nm) and eosin Y (λ_{max}~ 520 nm) photoinitiators compete for light with endogenous biological chromophores. This inner filter effect limits curing depths to just a few millimeters (1–5 mm) and increases curing variability in higher melanin skin types.[21] In short, current photoinitiators fail to take advantage of the so-called optical window of tissue (600–900 nm) where the absorption of hemoglobin, melanin (<600 nm), and water (>950 nm) is minimal.[23] Indeed, photons in the 600–900 nm wavelength range are used at clinically relevant centimeter depths for photodynamic therapy[24] and fluorescence guided surgery,[25] since they more readily transmit through tissue than shorter wavelengths. Biocompatible photoinitiators that undergo homolytic bond cleavage within this window are limited to inefficient two-photon activated groups that can only cure relatively small areas.[26,27] Burdick and co-workers reported near-infrared (NIR) initiation of thermal initiators with excited gold nanorods, but thermal initiation can be slow and the high temperatures required (~55 °C) can be detrimental to surrounding tissue and potential cellular cargo.[28] Consequently, the development of single photon, red light responsive photoinitiators would greatly improve transdermal photo-polymerization as a viable technique for in situ cured hydrogels.

Any photoresponsive molecule used to generate radicals within the desired 600–900 nm range must have a relatively low bond dissociation energy (~30–50 kcal/mol), thereby eliminating carbon–carbon and most carbon heteroatom bonds (C–O, C–N) as scissionable

motifs.[29] Recently, we reported the NIR induced scission of weak cobalt–carbon bonds present in vitamin B_{12}-derived alkyl-cobalamins (Co–C; bond dissociation energy ~ 30 kcal/mol).[30,31] Normally, excitation of unmodified alkyl-cobalamins (λ_{ex} ~ 510 nm) induces a metal-to-ligand charge transfer that decays to a dissociative alkyl radical and cobalt(II) species with high quantum yields (Φ ~ 20–40%).[32] However, despite lacking absorption longer than 600 nm, alkyl-cobalamin photolysis in the red, far red, and NIR can be achieved by excitation of covalently linked or noncovalently associated fluorophores.[30,31] While the energy transfer mechanism remains to be resolved, our lab found a range of fluorophores serve as a long wavelength-capturing antennae that induce cobalamin bond cleavage with tissue penetrating light. We report herein that the photolysis of fluorophore-substituted ethyl-cobalamins at tissue friendly wavelengths furnishes an alkyl radical that serves as a general photoinitiator for a variety of hydrogel systems.

EXPERIMENTAL SECTION

Detailed procedures for the synthesis and characterization of cobalamin-based photoinitiators, including their photolysis behavior (electron paramagnetic resonance (EPR) studies and quantum yields), are provided in the Supporting Information.

Light-Induced Polymerization

Acrylamide (1.6 M), *N*,N′-methylenebis(acrylamide) (10 mM), and photoinitiator (200 μM) were dissolved in DI water (400 μL), placed in a septum sealed vial (2 mL, 12 × 32 mm), and then degassed for 20 min with Ar. Samples were left in the dark or exposed unidirectionally to a Xe flash lamp (5–10 mW/cm^2) attenuated with bandpass filters (1″ diameter) at 546 ± 10, 646 ± 10, or 730 ± 10 nm for 5 min. Sample vials were inverted to determine successful gelation of the polymer solution. This procedure was repeated for the photopolymerization of polyethylene glycol diacrylate (PEGDA; 20 mM, M_n ~ 575 g/mol) and polyethylene glycol monomethyl acrylate (PEGMA; 200 mM, M_n ~ 480 g/mol).

Photolysis through Fitzpatrick Skin Models

Melanin was dissolved in a solution of NH_4OH (100 mM) to form a melanin stock solution (3 mg/mL). Hematocrit lysate stock solution (50% hematocrit) was prepared via sonicated lysis of erythrocytes in PBS. The sonicated solution was then centrifuged and filtered to remove residual membranes. All skin phantom solutions (3 mL) contained 3% v/v Intralipid and erythrocyte lysate solution (10% v/v). Melanin stock was added at varying concentrations depending on Fitzpatrick skin type (I –II ~8.8 μg/mL; III–IV ~66.0 μg/mL; V–VI ~130.0 μg/ mL). Initiator solutions of either **1** or **2** (10 μM, 1 mL) were placed in a cuvette (path length = 1 cm), and a skin phantom solution (path length = 1 cm) in a darkened cuvette was inserted between the initiator solution and light source. A 520 nm laser (2.4 mW/cm^2) was paired with **1**, and a 660 nm laser (2.2 mW/cm^2) was paired with **2**. A PerkinElmer UV–vis spectrometer was used to monitor the rate of initiator photolysis by analyzing the change in absorbance at 350 nm (Figure S3). Water and Intralipid (3 v/v%) solutions were used as control solutions to determine effects of light scattering on photolysis.

HepG2 Cell Encapsulation in PEG Hydrogels

Initiation with 1 or Irgacure 2959—Encapsulation by photopolymerization was performed at room temperature under aerobic conditions. HepG2 cells were trypsinized (0.25 v/v% trypsin-EDTA), pelleted by centrifugation, and washed (2 × 5 mL PBS). Cells were resuspended in PBS containing fibronectin (0.033 mg/mL) at a density of 3×10^6 cells/mL. A 30 μL aliquot of the resulting HepG2-fibronectin stock solution was combined with 70 μL of PEGDA (M_n ~3400 g/mol)/ initiator solution to a final volume of 100 μL. Final solution concentrations were 100 mM PEGDA, 9.9 μg/mL fibronectin, and 1 mM initiator. The solution was placed in a 35 mm Mattek dish well and covered with a coverslip. Polymer solutions containing Irgacure 2959 or **1** were illuminated at 350 ± 10 nm (12.8 mW/cm^2) or 546 nm ±10 nm (21.6 mW/cm^2), respectively, for 5 min. Following photopolymerization, the hydrogel was washed with PBS (3 × 1 mL). After washing, fresh media (L-15 + 10% FBS) was added, and the hydrogel returned to the 37 °C incubator for 30 min. The sample was covered with MEM alpha media (10% FBS/1% Pen-Strep) and incubated for 24 h (5% CO_2/95% humidity) before proceeding to the Live/Dead assay.

Initiation with 2—Photopolymerization was again performed under aerobic conditions at room temperature. HepG2 cells were trypsinized (0.25 v/v% trypsin-EDTA), pelleted by centrifugation, and washed (2 × 5 mL PBS). Cells were resuspended in PBS containing fibronectin (0.033 mg/mL) at a density of 3×10^6 cells/mL. A 46 μL aliquot of the resulting solution was combined with 50 μL of PEGDA solution (200 mM stock), 2.5 μL **2** solution (20 mM stock), and 2 μL bovine serum albumin solution (BSA, 10 mg/mL). Final solution concentrations were 100 mM PEGDA, 9.9 μg/mL fibronectin, 200 μg/mL BSA, and 500 μM **2**. The solution was placed in a 35 mm Mattek dish well and polymerized using two 660 nm LEDs (100 mW/ cm^2, 20 min exposure) positioned above and below the dish. Cells were cooled during polymerization using a small fan. Washing, incubation, and staining protocol for **1** and Irgacure 2959 was repeated for gels polymerized with **2**.

RESULTS AND DISCUSSION

Photoinitiators 1 and 2

Design, Synthesis, and Comparative Photophysical Properties—The photoinitiators **1** and **2** were prepared from vitamin B_{12} (cyanocob(III)alamin; **3**, Scheme 1). The latter is readily functionalized at both the Co and the ribose 5′-hydroxyl. The ribose alcohol of **3** was initially converted to the activated ester with 1,1-carbonyl-ditriazole (CDT) which, upon reaction with ethylenediamine, furnished a primary amine functional handle through a carbamate linkage (**4**, Scheme 1).[33] For our initial studies, we chose ethyl-cobalamin (EtCbl) due to its reported high quantum yield of photohomolysis (~0.3),[32] but it may be possible to use other primary alkyl ligands, such as aminopropyl, for dual photopolymerization and functionalization of hydrogels.[30,31] The EtCbl-ethylenediamine **5** intermediate is derived from Zn-mediated reduction of **4** to a supernucleophilic Co^I species and subsequent alkylation with ethyl bromide.[34] Photoinitiator **1** ($\varepsilon \sim 8500\ M^{-1}cm^{-1}$, $\lambda_{max} \sim$ 510 nm, Figure 1) was prepared by reacting the free amine of **4** with acetic anhydride. **1** extends the photoinitiator toolbox into the visible range, since examples of type I photoinitiators sensitive to light longer than 420 nm are limited.[35] Photoinitiator **2** was

synthesized via modification of the free amine in **4** with the NHS ester of Cy5, and it extends the photoinitiator toolbox deep into the red (λ_{max} ~ 646 nm, ε ~ 250 000 $M^{-1}cm^{-1}$, Figure 1).

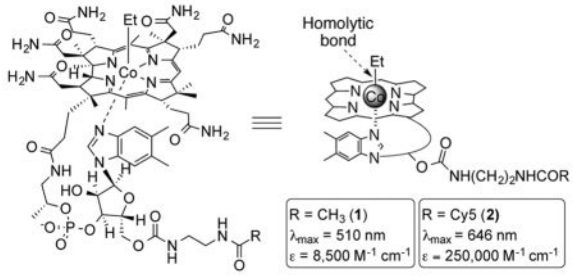

The normalized absorption spectra of **1** and **2** relative to that of tissue chromophores melanin and hemoglobin are shown in Figure 1a. Both melanin and hemoglobin absorb light from the short visible up to 600 nm. The common photoinitiators Irgacure and eosin Y display their maximal absorbance in this region (300–520 nm) (Figure 1b). We note that **1** absorbs modestly at green wavelengths (~510 nm) whereas **2** produces a much stronger absorption band at 646 nm. Like eosin Y, the absorbance of **1** significantly overlaps with melanin and hemoglobin. By contrast, the absorbance of **2** resides well within the optical window of tissue and outside of the reach of hemoglobin and melanin.

Wavelength Dependent Photolysis and Quantum Yield Determination

We investigated the wavelength dependent photolysis of **1** and **2** by illuminating samples (10 μM) at 546 ± 10, 646 ± 10, and 730 ± 10 nm using a Xe flash lamp (5–10 mW/cm^2). As determined by liquid chromatography–mass spectroscopy (LC-MS, Figures S4 and S5), both **1** and **2** are stable in the dark or when exposed to 730 nm as exemplified by the absence of the primary photobyproduct, hydroxocobalamin (**6**; CblOH, Co^{3+} oxidation state). However, both photoiniators form the photoproducts **6** when excited at the common 546 nm absorption band. By contrast, only **2** suffers photolysis to **6** when exposed to 646 nm, indicating successful photolysis-tuning to Cy5's primary absorption band (Figure S5).

These results are consistent with the notion that homolytic cleavage and ethyl radical production occurs at the green and red wavelengths.[30] We explicitly examined this conjecture using electron paramagnetic resonance (EPR) spectroscopy in combination with phenyl-*N*-*t*-butylnitrone (PBN) as a spin trap to detect wavelength dependent ethyl radical production (**7**).[36] In the dark, both **1** and **2** fail to produce any signal arising from paramagnetic species indicating Co–C bond stability in the absence of light. At 520 nm, both photoinitiators produce spectra with the expected splitting pattern of triplet of doublets (Table 1, Figure S6), as well as hyperfine couplings (a^N ~ 16.2–16.3 G, $a^{\beta\text{–H}}$ ~ 3.34) that compare favorably to reported ethyl-PBN adducts (a^N ~ 16.3, $a^{\beta\text{–H}}$ ~ 3.4).[36] By contrast, only **2** generates the expected splitting pattern with similar hyperfine constants (a^N ~ 16.2 G, $a^{\beta\text{–H}}$ ~ 3.34 G) at 660 nm illumination, consistent with radical production at wavelengths deep within the optical window of tissue.

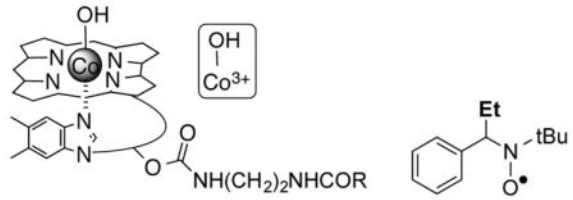

6 (R = Me or Cy5) **7**

For photoinitiators to induce rapid gelation times, the rate of radical production must be sufficiently high to allow for complete homolysis within seconds to several minutes, which necessitates a high extinction coefficient and quantum yield of homolysis (Co–C scission per photon absorbed, Φ_{hom}). By transient absorption, alkyl-cobalamins photolyze at 510 nm (α/β band) with near quantitative yields, but radical recombination within a solvent cage reduces the observed quantum yield to 20–30%.[32,37] This Φ_{hom} is comparable to the reported quantum yields of other common initiators, such as ~29% for Irgacure 2959 (I2959, λ_{max} < 300 nm) and ~25% for eosin Y/ triethanolamine (λ_{max} ~ 510 nm, 20 mM amine coinitiator) system.[38,39] We investigated the Φ_{hom} of both initiators exposed to 520 or 660 nm light with a constant photon flux (1 mW/ cm^2, Table 1, 2Figure 2). Both initiators photolyze at nearly identical rates at 520 nm, but the quantum yield of is reduced (Φ_{hom} ~ 14.8 ± 0.3%) relative to **1** (Φ_{hom} ~ 28.6 ± 1.7%) since **2** absorbs more photons at this wavelength (Table 1). The higher optical density of **2** also has a significant effect on the Φ_{hom} at 660 nm (Φ_{hom} of 7.4 ± 0.4%). However, the greater photon absorption of **2** enhances its photolytic rate and efficiency ($\varepsilon\Phi_{hom}$) relative to **1** at 520 nm (Figures 1 and 2, Table 1).

Photopolymerization of Acrylates

We determined the efficacy of cobalamin-initiated polymerization with acrylated monomers using ^{1}H NMR (Scheme S6, Table 2). Both photoinitiators **1** and **2** provide efficient monomer conversions at 520 nm. However, only compound **2** serves as an initiator of polymerization at 660 nm. Neither initiator induced monomer conversion when left in the dark (not shown). When polymerization was carried out in the presence of a bifunctional cross-linker (*N*,*N*′-methylenebis(acrylamide) or PEG-diacrylate, M_n ~ 575 g/mol), rapid gelation (<5 min) occurs with the expected wavelength dependence (Figure 3). As the inverted samples demonstrate, neither **1** nor **2** induces gelation in the dark or at 730 nm. However, both compounds effectively induce hydrogel formation upon exposure to 520 nm. In addition, exposure of prepolymer solutions of **2** to 660 nm likewise rapidly generates hydrogels. To ensure that the alkyl-cobalt bond scission is the primary factor in inducing gelation, hydroxocobalamin, Cy5, or a combination of both was used as control initiator (Figure S7). No gelation results at 520 or 660 nm, eliminating the possibility of thermal or photosensitization mechanisms to induce cross-linking.[40]

We investigated how cobalamin initiators affected gel cross-linking by determining the mass swelling ratio (W_{wet}/W_{dry}) of gels photopolymerized by **1** or the conventional UV initiator, I2959, over a range of cross-linker concentrations (Figure 4). The mass ratio is roughly correlated to the density of cross-links within the polymer network.[41] For example, lower

cross-linking density increases the mass of water retained at equilibrium as there is less elastic resistance within the polymer network to compete with water solvation. This provides a metric for comparison between the relative cross-linking density of gels. We calculated the ratio by measuring the weight of gels (~1 cm diameter) swollen with water to equilibrium (~24 h) and then dividing by the dry polymer weight after solvent removal and lyophilization. As expected, the ratios for both initiators decreased with increasing cross-linker concentration, but I2959 gave consistently lower ratios, especially at very low cross-linker concentrations. This indicates a higher amount of cross-linking relative to **1**, necessitating higher concentrations of cross-linker to achieve similar gel properties when using cobalamins.

Encapsulated Cell Viability

Hydrogels are indispensable as dynamic tissue scaffolds for implanted cells and tissue regeneration.[1,3,4] Therefore, cellular encapsulation within polymer networks requires mild gelation conditions to allow for high cell seeding. With this in mind, we determined the cytocompatibility of both cobalamin initiators compared to the commonly used I2959 by encapsulating HEPG2 cells (10^5 per gel) within PEG-diacrylate gels (M_n ~ 3400 g/mol, 100 mM). Viability was determined by *Z*-stack cell counting after imaging encapsulated cells with a confocal microscope using a standard LIVE/DEAD stain (Figure 5, Figure S8). Cells exposed only to light (>300, 520, or 660 nm), **1**, or solutions of PEGDA and **1** in the dark showed similar survival rates when compared to cells receiving no treatment (Figure 5b). However, when PEGDA polymerization was initiated with light at each initiator's (1 mM) primary excitation under aerobic conditions, all three displayed comparable viabilities [Irgacure 2959 (~76%), **1** (~81%), and **2** (~77%)]. Significant viability ensures that proliferation and seeding can be adjusted accordingly to the desired cell population. Others have noted that the cell line, the initiator, and the monomer composition can lead to variability in cell viability, suggesting that each situation will likely require some optimization to achieve desired gel properties and cellular cargo loading.[42]

Photolysis through a Dermal Tissue Model

Finally, we sought to demonstrate the utility of using red light initiation to activate photoinitiators through a dermal tissue model. Biochromophore concentration, particularly melanin, can fluctuate by body region and patient, producing variability in photon transmittance and curing.[43] As noted above, wavelengths shorter than the optical window of tissue are defined by their significant absorbance by biochromophores. As expected, this behavior is exacerbated by increasing biochromophore concentrations (Figure S9). Furthermore, light transmission through tissue is rendered even more challenging due to light scattering, with shorter wavelengths scattering more significantly than longer ones. As a consequence of both factors, green light sensitive eosin Y systems used in transdermal curing are limited to low melanin skin types (Fitzpatrick I–II) and show reduced effectiveness with darker skin types (Fitzpatrick type III and greater).[22] To test if red light induces photolysis of **2** through "dermal" tissue, we used skin phantom solutions as optical models for dermal tissue (Figure 6).[43] These phantom solutions contain Intralipid (3 v/v%), an emulsion of soybean oil commonly used in dermatology studies to mimic the light scattering properties of tissue.[43,44] In addition, these phantoms contain constant

concentrations of hemoglobin (10% hematocrit) but, to represent a variety of skin types, vary in melanin concentration ranging from 8.8 μg/mL (pale skin, Fitzpatrick type I–II) to 130 μg/mL (dark skin, Fitzpatrick type V–VI).

Initiator solutions (10 μM) of **1** and **2** were irradiated using weak lasers (520, 2.4 mW/cm^2 for **1** or 660 nm, 2.2 mW/cm^2 for **2**) passed through skin phantom solutions in a cuvette (path length ~ 1 cm). Conversion to the CblOH-1,2 (**6**) photo-products was monitored by UV/vis spectroscopy (Figure S3). As expected, control solutions containing only water showed rapid photolysis of both **1** (52.5 nM/s) and **2** (64.5 nM/s) due to limited light attenuation. However, Intralipid (3 v/v %) solutions alone lowered the photolysis rate of both initiators presumably due to light scattering, but a moderate rate was still noted for both **1** and **2** (Figure 6b, 7.7 and 13.0 nM/s, respectively). Light scattering is a potential challenge for all phototherapies, but this limitation is typically overcome in photodynamic therapy by increasing light dosage and irradiation diameter.[45]

When hemoglobin lysate (10 v/v%) and a small amount of melanin were introduced into the phantom solution ([melanin] ~ 8.8 μg/mL, Fitzpatrick type I–II), **1** failed to photolyze even after 30 min of 520 nm illumination. Photoinitiator **1** photolyzes in the same range as eosin Y's activation wavelength (λ_{max} ~ 500 nm), implying photoactivation of any green light initiator may suffer when light encounters Fitzpatrick type I–II skin. On the other hand, **2** suffers photolysis at a similar rate when 660 nm light is passed through either Fitzpatrick type I–II (16.3 nM/s, [melanin] ~ 8.8 μg/mL) or type III–IV (16.7 nM/s, [melanin] ~ 66 μg/mL) solution. At very high melanin concentrations (130 μg/mL, Fitzpatrick type V–VI), the photolysis rate does drop (10.6 nM/s) but still remains robust. Therefore, extension of the photolysis wavelength to 660 nm may allow for broader applicability of transdermal photocuring in higher melanin containing skin types. This effect may be extended farther into the far red and near-infrared through use of a longer wavelength fluorophore absorbing in a region where biochromophore absorption is effectively zero and light scattering is reduced.[30,31]

CONCLUSIONS

We have demonstrated that light-induced hydrogel formation can be mediated by alkyl-cobalamin-based photoinitiators. Furthermore, we have shown that the wavelength of photo-initiation can be extended from green to red by simply appending a red light-absorbing chromophore. Photoinitiation proceeds via radical formation with good quantum yields and in demanding dermal tissue models. These properties suggest that alkyl-cobalamins should find utility for noninvasive hydrogel cell implantation by furnishing greater curing depths and limiting curing variability in higher melanin containing skin types. As a consequence, alkyl cobalamin photoinitiators could find utility in medical conditions that range from damaged cartilage[8,13] to glioblastoma.[46]

Supplementary Material

Refer to Web version on PubMed Central for supplementary material.

Acknowledgments

We thank Weston Smith for his construction of the LED and laser sources used during this investigation. We thank the National Institutes of Health (R01 CA79954) for financial support.

References

1. Van Vlierberghe S, Dubruel P, Schacht E. Biomacromolecules. 2011; 12:1387–1408. [PubMed: 21388145]
2. Seliktar D. Science. 2012; 336:1124–1128. [PubMed: 22654050]
3. Elisseeff J, Puleo C, Yang F, Sharma B. Orthod Craniofacial Res. 2005; 8:150–161.
4. Baroli B. J Pharm Sci. 2007; 96:2197–2223. [PubMed: 17593553]
5. Nguyen KT, West JL. Biomaterials. 2002; 23:4307–4314. [PubMed: 12219820]
6. Perale G, Rossi F, Sundstrom E, Bacchiega S, Masi M, Forloni G, Veglianese P. ACS Chem Neurosci. 2011; 2:336–345. [PubMed: 22816020]
7. Davis ME, Hsieh PCH, Grodzinsky AJ, Lee RT. Circ Res. 2005; 97:8–15. [PubMed: 16002755]
8. Sharma B, Fermanian S, Gibson M, Unterman S, Herzka D, Cascio B, Coburn J, Hui AY, Marcus N, Gold GE, Elisseeff JH. Sci Transl Med. 2013; 5:167ra6.
9. Xu X, Weng Y, Xu L, Chen H. Int J Biol Macromol. 2013; 60:272–276. [PubMed: 23748006]
10. Lin CC, Anseth KS. Pharm Res. 2009; 26:631–643. [PubMed: 19089601]
11. Van Tomme SR, Storm G, Hennink WE. Int J Pharm. 2008; 355:1–18. [PubMed: 18343058]
12. Page JM, Harmata AJ, Guelcher Sa. J Biomed Mater Res, Part A. 2013; 101:3630–3645.
13. Elisseeff J. Expert Opin Biol Ther. 2004; 4:1849–1859. [PubMed: 15571448]
14. Patenaude M, Smeets NMB, Hoare T. Macromol Rapid Commun. 2014; 35:598–617. [PubMed: 24477984]
15. Alexander A, Ajazuddin Khan J, Saraf S, Saraf S. Eur J Pharm Biopharm. 2014; 88:575–585. [PubMed: 25092423]
16. Singh NK, Lee DS. J Controlled Release. 2014; 193:214–227.
17. Huynh CT, Nguyen MK, Lee DS. Macromolecules. 2011; 44:6629–6636.
18. Fisher JP, Dean D, Engel PS, Mikos AG. Annu Rev Mater Res. 2001; 31:171–181.
19. Ifkovits JL, Burdick JA. Tissue Eng. 2007; 13:2369–2385. [PubMed: 17658993]
20. Hoffmann JC, West JL. Integr Biol. 2013; 5:817–827.
21. Elisseeff J, Anseth K, Sims D, McIntosh W, Randolph M, Anger RL. Proc Natl Acad Sci U S A. 1999; 96:3104–3107. [PubMed: 10077644]
22. Hillel AT, Unterman S, Nahas Z, Reid B, Coburn JM, Axelman J, Chae JJ, Guo Q, Trow R, Thomas A, Hou Z, Lichtsteiner S, Sutton D, Matheson C, Walker P, David N, Mori S, Taube JM, Elisseeff JH. Sci Transl Med. 2011; 3:93ra67.
23. Smith AM, Mancini MC, Nie S. Nat Nanotechnol. 2009; 4:710–711. [PubMed: 19898521]
24. Szaciłowski K, Macyk W, Drzewiecka-Matuszek A, Brindell M, Stochel G. Chem Rev. 2005; 105:2647–2694. [PubMed: 15941225]
25. Nguyen QT, Tsien RY. Nat Rev Cancer. 2013; 13:653–662. [PubMed: 23924645]
26. Lee KS, Kim RH, Yang DY, Park SH. Prog Polym Sci. 2008; 33:631–681.
27. Li L, Fourkas JT. Mater Today. 2007; 10:30–37.
28. Gramlich WM, Holloway JL, Rai R, Burdick JA. Nanotechnology. 2014; 25:014004. [PubMed: 24334436]
29. Halpern, J. Bonding Energetics in Organometallic Compounds. Marks, TJ., editor. American Chemical Society; Washington DC: 1990. p. 100-122.
30. Shell TA, Shell JR, Rodgers ZL, Lawrence DS. Angew Chem, Int Ed Engl. 2014; 53:875–878. [PubMed: 24285381]
31. Smith WJ, Oien NP, Hughes RM, Marvin CM, Rodgers ZL, Lee J, Lawrence DS. Angew Chem, Int Ed Engl. 2014; 53:10945–10948. [PubMed: 25154925]

32. Taylor RT, Smucker L, Hanna ML, Gill J. Arch Biochem Biophys. 1973; 156:521–533. [PubMed: 4718782]
33. Lee M, Grissom CB. Org Lett. 2009; 11:2499–2502. [PubMed: 19441855]
34. Smeltzer CC, Cannon MJ, Pinson PR, Munger JD, West FG, Grissom CB. Org Lett. 2001; 3:799–801. [PubMed: 11263885]
35. Fairbanks BD, Schwartz MP, Bowman CN, Anseth KS. Biomaterials. 2009; 30:6702–6707. [PubMed: 19783300]
36. Augusto O, Ortiz de Montellano PR, Quintanilha A. Biochem Biophys Res Commun. 1981; 101:1324–1330. [PubMed: 6272782]
37. Peng J, Tang K, McLoughlin K, Yang Y, Forgach D, Sension RJ. J Phys Chem B. 2010; 114:12398–12405. [PubMed: 20815360]
38. Jockusch S, Landis MS, Freiermuth B, Turro NJ. Macromolecules. 2001; 34:1619–1626.
39. Encinas MV, Rufs AM, Bertolotti SG, Previtali CM. Polymer. 2009; 50:2762–2767.
40. Dika I, Malval JP, Soppera O, Bardinal V, Barat D, Turck C, Spangenberg A, Bruyant A. Chem Phys Lett. 2011; 515:91–95.
41. Peppas NA, Huang Y, Torres-Lugo M, Ward JH, Zhang J. Annu Rev Biomed Eng. 2000; 2:9–29. [PubMed: 11701505]
42. Williams CG, Malik AN, Kim TK, Manson PN, Elisseeff JH. Biomaterials. 2005; 26:1211–1218. [PubMed: 15475050]
43. Smit JE, Grobler AF, Sparrow RW. Photochem Photobiol. 2011; 87:64–71. [PubMed: 21073475]
44. Karsten AE, Smit JE. Photochem Photobiol. 2012; 88:469–474. [PubMed: 22077284]
45. Dominguez EA, Bar-Sela A, Musher DM. Rev Infect Dis. 2012; 9:1193–1201. [PubMed: 3321368]
46. Kauer TM, Figueiredo JL, Hingtgen S, Shah K. Nat Neurosci. 2012; 15:197–204. [PubMed: 22197831]

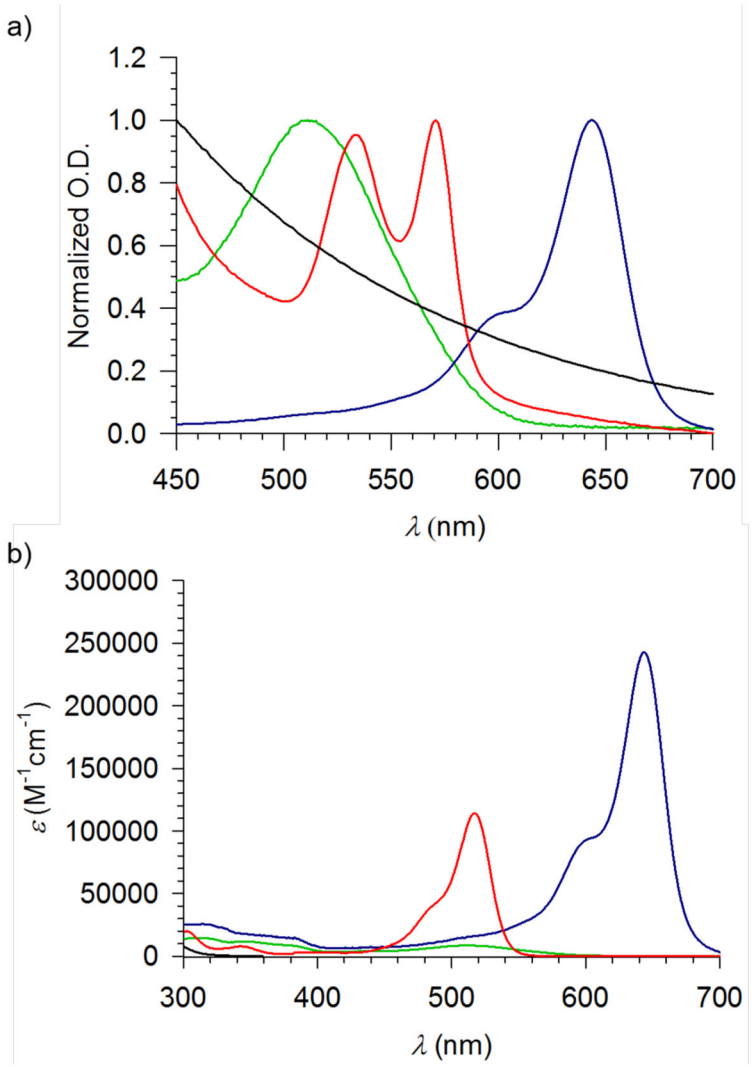

Figure 1.

(a) Normalized visible spectra of **1** (green) and **2** (blue) relative to melanin (black) and hemoglobin (red). (b) Absorption spectra of photoinitiators **1** (green), **2** (blue), eosin Y (red), and Irgacure 2959 (black).

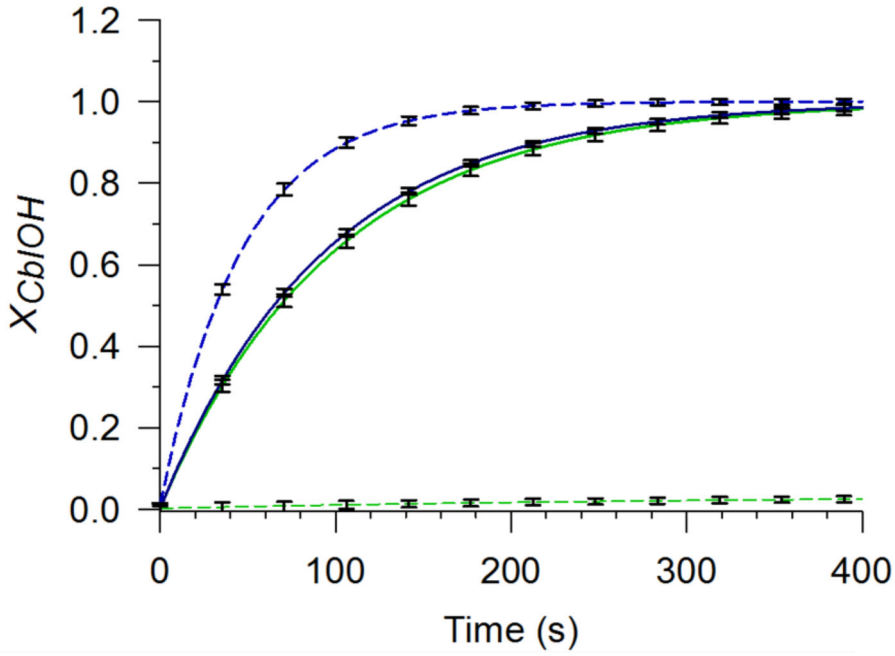

Figure 2.

Mole fraction of **1** (green) and **2** (blue) converted to hydroxocobalamin (X_{CblOH}) versus irradiation time by a 520 nm (solid line) or 660 nm (dashed line) laser.

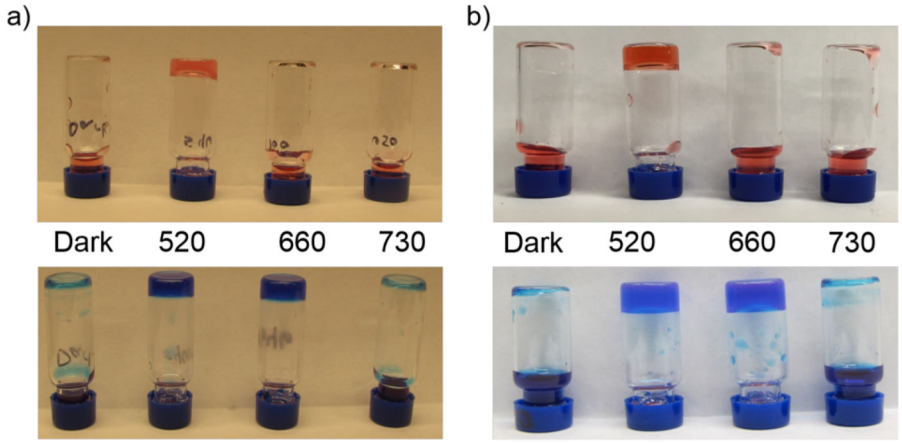

Figure 3.

Wavelength dependent gelation of (a) acrylamide (1.6M) and bis(acrylamide) (10 mM) or (b) PEG-monoacrylate (M_n ~ 480 g/mol, 200 mM) and PEG-diacrylate (M_n ~ 575 g/mol, 20 mM). Samples were left in the dark or irradiated at 520, 660, or 730 nm using **1** (top) or **2** (bottom) initiators.

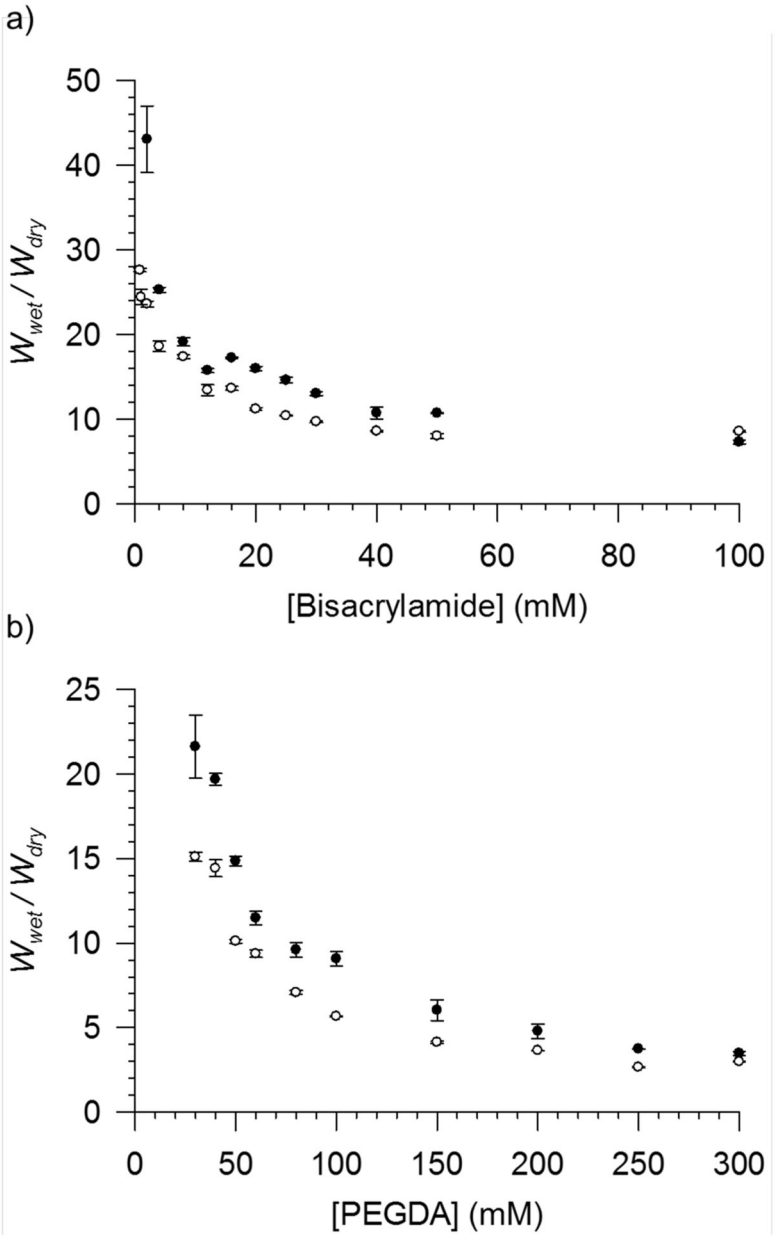

Figure 4.

(a) Acrylamide/bis(acrylamide) and (b) PEG-monoacrylate/PEG-diacrylate hydrogel wet/dry weight ratios with varying bifunctional cross-linker concentrations using 200 μM **1** (●) or Irgacure 2959 (○) initiators irradiated at 520 nm or <300 nm, respectively.

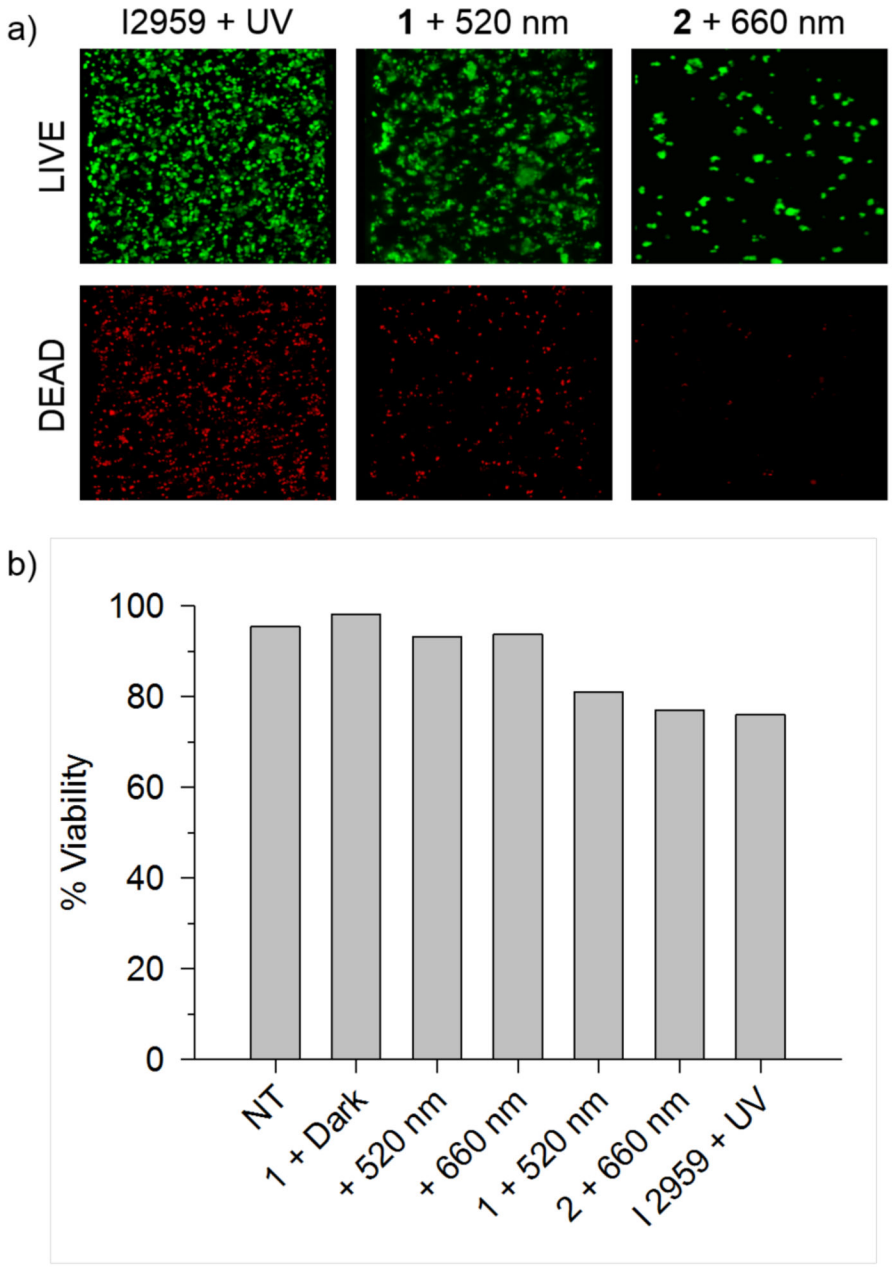

Figure 5.

(a) LIVE/DEAD images of encapsulated HepG2 cells within PEG-diacrylate (M_n ~ 3400 g/mol, 100 mM) hydrogels using Irgacure 2959 (I2959), **1**, or **2** and corresponding exciting wavelength as initiators. b) Cell viability of encapsulated HepG2 cells determined by simple cell counting. NT indicates no treatment.

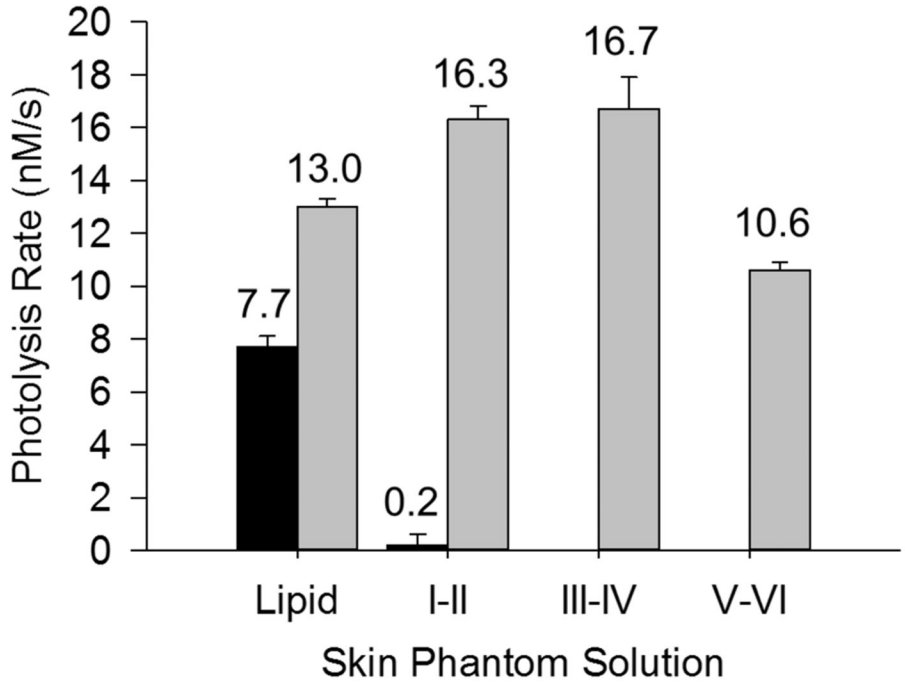

Figure 6.

"Transdermal" photolysis rate of initiators with various Fitzpatrick skin type phantoms. **1** (black bars) was photolyzed with a green 520 nm (2.4 mW/cm^2) laser, and **2** (gray bars) with a red 660 nm laser (2.2 mW/cm^2).

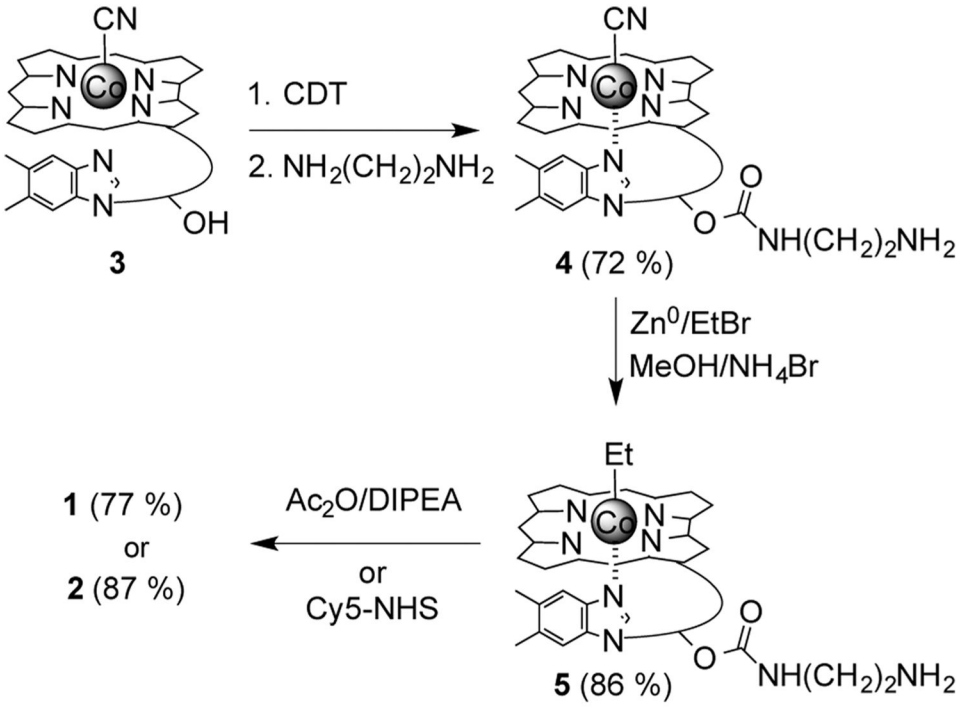

Scheme 1.
Synthesis of Et-Cbl Initiators 1 and 2

Table 1

Photochemical Properties and Hyperfine Couplings from Et-Cbl Initiator Photolysis

initiator	λ (nm)	Φ_{hom} (%)	$\varepsilon\Phi_{hom}$ (M^{-1} cm^{-1})[a]	a^N (g)	$a^{\beta\text{-H}}$ (g)
EtCbl[b]	520	20–30	~2000	16.3	3.4
	660	NR	NR	NR	NR
1	520	28.6 ± 1.7	2366	16.3	3.3
	660	*c*	*c*	*c*	*c*
2	520	14.8 ± 0.3	2405	16.2	3.3
	660	7.4 ± 0.2	9435	16.2	3.3

[a] Product of the ε and Φ where $\varepsilon \sim 8275$ M^{-1} cm^{-1} (**1** @ 520 nm); 16 250 M^{-1} cm^{-1} (**2** @ 520 nm); 127 500 M^{-1} cm^{-1} (**2** @ 660 nm).

[b] From ref 32. NR = not reported.

[c] No detectable conversion.

Table 2

Photoinitiated Monomer Conversion Using Cobalamin Initiators

		conversion % by λ^c		
initiator[a]	**monomer**[b]	**<300 nm**	**520 nm**	**660 nm**
1	acrylamide	89	90	*d*
	acrylic acid	93	93	15
	N-isopropylacrylamide	93	96	*d*
	hydroxyethyl acrylate	86	88	2
	PEG-monoacrylate	89	88	*d*
2	acrylamide	27	27	56
	acrylic acid	87	59	72
	N-isopropylacrylamide	89	92	71
	hydroxyethyl acrylate	64	69	80
	PEG-monoacrylate	61	74	80

[a] [Initiator] = 200 μM.

[b] [Monomer] = 1 M in D_2O

[c] Determined by ^1H NMR

[d] Indicates no detectable conversion.